

miR-192-5p Silencing by Genetic Aberrations Is a Key Event in Hepatocellular Carcinomas with Cancer Stem Cell Features



Yuanzhuo Gu¹, Xiyang Wei¹, Yulin Sun², Hongjun Gao^{3,4}, Xin Zheng⁵, Linda L. Wong^{3,6}, Ling Jin³, Niya Liu¹, Brenda Hernandez³, Karolina Peplowska³, Xiaohang Zhao², Qi-Min Zhan⁷, Xin-Hua Feng¹, Zhao-You Tang⁸, and Junfang Ji¹

Abstract

Various cancer stem cell (CSC) biomarkers have been identified for hepatocellular carcinoma (HCC), but little is known about the implications of heterogeneity and shared molecular networks within the CSC population. Through miRNA profile analysis in an HCC cohort ($n = 241$) for five groups of CSC⁺ HCC tissues, i.e., EpCAM⁺, CD90⁺, CD133⁺, CD44⁺, and CD24⁺ HCC, we identified a 14-miRNA signature commonly altered among these five groups of CSC⁺ HCC. miR-192-5p, the top-ranked CSC miRNA, was liver-abundant and -specific and markedly downregulated in all five groups of CSC⁺ HCC from two independent cohorts ($n = 613$). Suppressing miR-192-5p in HCC cells significantly increased multiple CSC populations and CSC-related features through targeting

PABPC4. Both *TP53* mutation and hypermethylation of the miR-192 promoter impeded transcriptional activation of miR-192-5p in HCC cell lines and primary CSC⁺ HCC. This study reveals the circuit from hypermethylation of the miR-192 promoter through the increase in PABPC4 as a shared genetic regulatory pathway in various groups of primary CSC⁺ HCC. This circuit may be the driver that steers liver cells toward hepatic CSC cells, leading to hepatic carcinogenesis.

Significance: miR-192-5p and its regulatory pathway is significantly abolished in multiple groups of HCC expressing high levels of CSC markers, which may represent a key event for hepatic carcinogenesis.

Introduction

Primary liver cancer is the second leading cause of cancer-related mortality worldwide, and approximately 90% of them are hepatocellular carcinoma (HCC; refs. 1, 2). Liver resection and liver transplantation are the only potential curative therapies; however, only 10% to 20% of patients with HCC are surgical candidates, and the chance of recurrence is significant. For inoperable patients, liver-directed locoregional therapy, systemic chemotherapy, or molecular therapy such as sorafenib may be offered with limited success, and their overall survival rate is poor (3, 4).

Cancer stem cells (CSC) are implicated in tumor initiation, tumor metastasis and recurrence, as well as in chemoresistance

(5, 6). Eradicating CSCs may achieve stable tumor remission. Multiple hepatic CSC biomarkers such as EpCAM, CD133, CD90, CD44, and CD24 have been used to enrich tumorigenic CSCs in primary HCCs (7–15). These different hepatic CSCs present similar "stem-like" characteristics including self-renewal, differentiation, increased invasion ability, as well as tumorigenicity in NOD/SCID mice, etc. (7, 11–18). Researchers have also investigated the underlying molecular signatures of individual hepatic CSC populations. For example, we previously found that Wnt/miR-181s/NLK signaling pathway was activated in EpCAM⁺ HCC cells (19, 20). In CD133⁺ hepatic CSCs compared with CD133⁻ cells, miR-130b was highly expressed, whereas miR-150 was reduced (12, 21). Interestingly, miR-150 was found to be highly expressed in EpCAM⁺ HCC cells (22), suggesting potential variations in the molecular signatures among these different hepatic CSC populations. However, little is known about the implication of CSC heterogeneity and presence of any shared molecular networks.

Further comparison of the molecular profiles of various types of CSC⁺ HCCs might pave the way for a better understanding of the implication of CSC heterogeneity. miRNAs, approximately 22-nt noncoding RNA molecules, are functionally linked to normal stem cells and CSCs as well as hepatic carcinogenesis (23–25). Thus, we selected five hepatic CSC biomarkers that have been verified in primary HCCs, i.e., EpCAM, CD90, CD133, CD44, and CD24 (7–12), to identify CSC⁺ HCC cases, and analyzed their miRNA profiles. We detected a group of consistently altered miRNAs in these different groups of CSC⁺ HCCs. miR-192-5p, the top candidate, was further explored for its expression, function, and regulation in HCCs. We revealed an axis of *TP53* mutation/miR-192 promoter

¹Life Sciences Institute, Zhejiang University, Hangzhou, Zhejiang Province, China.

²State Key Laboratory of Molecular Oncology, National Cancer Center/Cancer Hospital, Chinese Academy of Medical Sciences and Peking Union Medical College, Beijing, China.

³University of Hawai'i Cancer Center, Honolulu, Hawaii.

⁴Clinical Laboratory, China Meitan General Hospital, Beijing, China.

⁵EZKIT LLC, Honolulu, Hawaii.

⁶Department of Surgery, John A. Burns School of Medicine, University of Hawai'i, Honolulu, Hawaii.

⁷Key Laboratory of Carcinogenesis and Translational Research (Ministry of Education), Peking University Cancer Hospital and Institute, Beijing, China.

⁸Liver Cancer Institute and Zhongshan Hospital, Fudan University, Shanghai, China.

Note: Supplementary data for this article are available at Cancer Research Online (<http://cancerres.aacrjournals.org/>).

Y. Gu, X. Wei, Y. Sun, and H. Gao are the joint first authors of this article.

Corresponding Author: Junfang Ji, Zhejiang University, Hangzhou 310058, China. Phone: 86-571-8820-8956; E-mail: junfangji@zju.edu.cn

doi: 10.1158/0008-5472.CAN-18-1675

©2018 American Association for Cancer Research.

hype-methylation/reduced miR-192-5p/increased PABPC4 (target of miR-192-5p) in HCCs expressing high levels of CSC markers. These findings unraveled a genetic regulatory signaling pathway being shared by different CSC⁺ HCCs, which improved our current understanding of CSC heterogeneity as well as informed potential early diagnosis and/or molecular therapy for HCC.

Materials and Methods

HCC cohorts and corresponding omics datasets

A total of three cohorts and five corresponding profiling datasets were used (Supplementary Table S1). Cohort 1 included 241 Chinese HCC cases. Previous studies from this cohort have described HCC miRNA microarray dataset in paired HCC tumor and nontumor specimens (GSE6857; ref. 26). Among these HCC cases, mRNA microarray profiling was available in 176 HCC cases in both tumor and nontumors (GSE14520; refs. 27, 28), and *TP53* mutation status was available in 152 cases (29).

Cohort 2 included 372 HCC cases with 42% of Asian patients and 45% of Caucasian. miRNA sequencing data of 372 HCC tissues and 50 normal liver tissues were downloaded from The Cancer Genome Atlas (TCGA). Among them, mRNA deep sequencing data were available in 367 HCC tissues. Methylation 450K array data were available in 286 HCC tissues, among which, there were 242 with *TP53* mutation status (www.cbioportal.org/index.do).

Cohort 3 consisted of 53 patients with HCC, including 10 Caucasians, 34 Asians (Japanese, $n = 12$; Chinese, $n = 10$; Korean, $n = 5$; Filipino, $n = 4$; Vietnamese, $n = 3$), and other pacific islanders ($n = 9$). We used previously archived formalin-fixed paraffin-embedded (FFPE) HCC tissues from these patients (30). These were retrospectively-collected deidentified specimens and obtained from the Hawaii Tumor Registry Residual Tissue Repository of the National Cancer Institute Surveillance, Epidemiology, and End-Results program. The use of these specimens was approved as exempt research by the Institutional Review Board of the University of Hawaii. DNAs and RNAs isolated from these specimens were used for this study.

RNAs from 20 human organs, HCC cell lines, and FFPE tissues

RNAs from 20 human normal organs were purchased from Clontech, which included 18 adult organs and 2 fetal organs. Total RNAs from all HCC cell lines were extracted using the standard TRIzol method. Total RNAs from FFPE tissues were isolated via the MasterPure RNA Purification Kit (Epicentre) as we did before (31).

HCC cell lines, dual-luciferase assay, and 5-AZA treatment

Human liver cancer cell lines (HuH1, HuH7, Hep3B, SK-Hep1, HLE, and HLF) and 293T cells were routinely cultured in our lab as we described before (22). HuH1, HuH7, HLE, and HLF were originally from JCRB, whereas SK-Hep1, Hep3B, and 293T were from the ATCC. They were authenticated via short tandem repeat profile done by GTB Corporation. Cell lines were confirmed to be negative for *Mycoplasma* by a TransDetect PCR Mycoplasma Detection Kit (FM311-01, Transgen Biotech). Dual-luciferase assay for examining the miR-192-5p downstream targets was performed as we did previously (19, 22). When indicated, HLE, SK-Hep1, and HLF cells were treated for 3 days with 1, 2, and 10 $\mu\text{mol/L}$ 2'-deoxy-5-azacytidine (5-AZA; Sigma, #A3656).

DNA isolation, pyrosequencing, methylation-specific PCR, and Sanger sequencing

DNAs were isolated via the MasterPure DNA Purification Kit (Epicentre). One microgram of extracted DNA was used for bisulfite conversion using the EZ DNA Methylation Direct Kit (Zymo Research) following the standard procedure. Pyrosequencing analysis was done at the University of Hawaii Cancer Center Genomics Shared Resource. For methylation-specific PCR, methylation-specific primers (MSP) and unmethylation-specific primers (UMSP) were used, and PCR was performed in a final volume of 25 μL using Taq DNA polymerase (ThermoFisher Scientific) with 1 μL of bisulfite-converted template. For validating the methylation sites using Sanger-sequencing method, PCR was performed with high-fidelity DNA polymerase (ThermoFisher Scientific). All the primers were listed in Supplementary Table S2.

Proteomics analysis

HLF cells infected with lentivirus pmiR-192 and pmiR-control were used for proteomics analysis at the University of California Davis Proteomics Core Facility (32). The experiments were performed in triplicate. Briefly, 5×10^6 HLF cells were lysed, and protein was extracted for LC-MS/MS on a Thermo Scientific Q Exactive Orbitrap Mass spectrometer in conjunction with Waters UPLC and Proxeon nanospray source. Scaffold software (version Scaffold_4.0.6.1, Proteome Software Inc.) was used to validate MS/MS-based peptide and protein identifications. A total of 2,746 proteins were identified based on 1 peptide spectrum covering and were used to identify the downregulated proteins by miR-192-5p overexpression. One hundred and twenty-three proteins with known unique gene names were significantly decreased by miR-192-5p overexpression ($P < 0.05$) and used for further miR-192-5p target identification.

Sphere formation, colony formation, cell migration, cell invasion, wound-healing assay, and tumorigenicity assay

These assays were performed as we described previously (19, 22, 33) and also detailed in Supplementary File. For tumorigenicity assay, 6-week-old male BALB/c nude mice were purchased from SLAC Laboratory Animal Center. The protocols were approved by the Institutional Animal Care and Use Committee of Zhejiang University. Cells were suspended in 200 μL of DMEM and Matrigel (1:1), and s.c. injection was performed.

Statistical analysis

Hierarchical clustering analysis was performed by the GENESIS software version 1.7.6 developed by Alexander Sturn (IBMT-TUG). The Student *t* test, Mann-Whitney rank test, and one-way ANOVA were used for statistical analysis of comparative data between groups. The two-way ANOVA analysis was used to compare the migration ability of HCC cells in wound-healing assay at different time points. The Kaplan-Meier survival analysis was used to compare patient survival based on prediction results using Graphpad Prism V5.0, and the statistical *P* value was generated by the Cox-Mantel log-rank test. Pearson correlation was used to identify gene surrogates of related miR-192-5p. Pathway analysis was performed using Ingenuity Pathway Analysis V8.6. All *P* values were two-sided, and the statistical significance was defined as a *P* value of less than 0.05.

Results

miR-192-5p expressed at a significantly low level in five different groups of CSC⁺ HCC cases

To understand the implication of CSC heterogeneity in patients with HCC, we sought to compare molecular profiles of various types of CSC⁺ HCCs. We used available miRNA and mRNA transcriptome data in 176 HCCs from Cohort 1 and 367 HCCs from Cohort 2 (Supplementary Table S1). Five different hepatic CSC biomarkers were selected to identify CSC⁺ HCCs based on (1) validation by xenograft tumorigenicity assay using CSC marker-positive cells isolated from primary HCC tissues, and (2) use in more than two different research groups. These five selected markers were EpCAM, CD133, CD90, CD44, and CD24 (7–12, 17, 34). For each hepatic CSC marker, HCCs with the top quartile of expression levels in their tumors were identified as CSC⁺ HCCs (Cohort 1, $n = 44$; Cohort 2, $n = 92$), and the bottom quartile was CSC⁻ HCC as previously described (Fig. 1A; Supplementary Fig. S1A; ref. 22). Hierarchical analysis of the five CSC biomarkers showed that CSC⁺ HCCs with different markers did not cluster tightly (Supplementary Fig. S1B). In Cohort 1, only one HCC case was positive for the five markers, whereas limited cases were positive for three to four markers (4 markers, $n = 10$; 3 markers, $n = 16$). Consistent data were obtained from Cohort 2, with only five cases positive for all five markers. These indicate that HCCs positive for different CSC markers represent diverse populations.

MiRNA profiling comparisons between CSC⁺ and CSC⁻ HCCs for each biomarker were subsequently performed, followed by Venn Diagram analysis of the five miRNA signatures. Twenty-five probes (14 unique miRNAs) were significantly commonly downregulated in the five groups of CSC⁺ HCC cases (Fig. 1B). Interestingly, as key players in EpCAM⁺ HCCs, miR-181 family members (including miR-181a-5p, miR-181b-5p, and miR-181c-5p) were significantly upregulated not only in EpCAM⁺ HCCs but also in CD133⁺, CD24⁺, and CD90⁺ HCCs (Supplementary Fig. S1C). Supervised clustering further revealed that this 14-CSC miRNA signature classified patients with HCC into two groups. Patients with CSC⁺ HCC were enriched in one group with substantial low levels of these miRNAs (Fig. 1C). miR-192-5p was the top candidate based on its abundance and significance (Fig. 1B). In HCCs with a low level of miR-192-5p, CSC⁺ HCCs were also evidently gathered (Fig. 1C).

Both patients with lower levels of 14-CSC miRNAs in their tumors (group 1 in Fig. 1C), and those with lower levels of miR-192-5p in tumors, had a significantly worse overall survival and a shorter time interval to tumor recurrence (Fig. 1D and E; Supplementary Fig. S2A and S2B). The association of HCCs with a low level of miR-192-5p and poor prognosis was also validated in Cohort 3 (Supplementary Fig. S2C–S2F). Consistently, patients with HCC with lower level of miR-192 (precursor of miR-192-5p) also had shorter overall survival in Cohort 2 (35). In addition, we performed gene set enrichment analysis (GSEA) in the Molecular Signatures Database using miR-192-5p-correlated genes. Through Pearson correlation of the case-matched miRNA and mRNA microarray datasets in Cohort 1 as previously described (22), the top 5% of positively correlated genes ($n = 656$, $P < 0.001$) and top 5% of negatively correlated genes ($n = 655$, $P < 0.001$) were identified as miR-192-5p-related genes (Supplementary Fig. S1D). GSEA analysis of these genes revealed that miR-192-5p was positively related to good survival signatures, a low early recurrence signature, and genes with low levels in CSCs (Fig. 1F). Taken together, these results

indicate the presence of shared molecular networks among various CSCs.

miR-192-5p, a liver-specific and -abundant miRNA, was significantly downregulated in HCCs, especially in CSC⁺ HCCs

Consistent with results of mature miR-192-5p from Cohort 1, precursor miR-192 expressed at a significantly lower level ($P < 0.001$) in five CSC⁺ HCC groups compared with the corresponding CSC⁻ groups in Cohort 2 (Fig. 2A). Both mature miR-192-5p (Cohort 1) and precursor miR-192 (Cohort 2) also displayed a significantly lower level in other hepatic CSC marker-positive HCCs [i.e., OV6⁺ (or CXCR4⁺), CK19⁺, and DCLK1⁺ HCCs] as well as pluripotency marker-positive HCCs (i.e., SOX2⁺, KLF4⁺, Nanog⁺ HCCs; Supplementary Fig. S3A and S3B). In addition, both miR-192-5p and its precursor were highly conserved among various species (Supplementary Fig. S3E and S3F).

Our data further indicated that miR-192-5p was a liver-abundant and liver-specific miRNA. In our archived RNA-sequencing data from hepatocytes (22), 17.4% of reads were miR-192-5p, the second highest abundant miRNA among 1,231 identified miRNAs (Fig. 2B, left plot). In nontumor liver tissues of Cohort 2, miR-192 was ranked as the fifth highest miRNA (Fig. 2B, right plot). Meanwhile, qRT-PCR analysis of miR-192-5p expression among 18 different human adult normal organs revealed the highest level of miR-192-5p in the liver tissue compared with that in other tissues (Fig. 2C). Consistently, the precursor miR-192 showed the highest level in the liver among 17 available nontumor tissue RNA sequencing datasets (Fig. 2D).

Interestingly, miRNA array data from Cohort 1 presented a significant downregulation of mature miR-192-5p in HCCs in comparison with non-HCCs (Fig. 2E). The qRT-PCR data in HCCs (Cohort 3, $n = 53$) also revealed a reduced level of miR-192-5p in 42 of 53 HCCs compared with normal adult livers (Fig. 2E). Consistently, Lian and colleagues reported the downregulation of precursor miR-192 in HCCs of Cohort 2 (35), which was also shown in our Fig. 2E. The data from three different technologies utilizing 666 HCC cases with various etiologies and ethnicities consistently presented downregulation of miR-192-5p in HCC tumors compared with that in nontumor livers.

We further explored its downregulation in HCCs with different expression levels of CSC biomarkers. Strikingly, the significant downregulation of miR-192-5p and its precursor miR-192 did not occur in most of CSC⁻ HCC groups (four groups in Cohort 1 and five groups in Cohort 2), but in all groups of CSC⁺ HCC cases (Fig. 2F, $P < 0.001$ for each comparison) and in the remaining HCC cases with P values ranging from 0.04 to < 0.001 from both cohorts. Together, we reasoned that the low expression of miR-192-5p was a key feature among various groups of CSC⁺ HCCs.

miR-192-5p significantly suppressed the CSC-related features in HCC cell lines

To investigate the roles of miR-192-5p in regulating hepatic CSC features, we used *in vitro* systems to suppress or overexpress miR-192-5p in HCC cell lines. Among six commonly used HCC cell lines, HuH7, HepG2, and HuH1 cells expressed >20-fold higher levels of miR-192-5p compared with HLF, HLE, and SK-Hep1 (Fig. 3A). HuH7 and HepG2 cells infected with lentivirus miRZip-192 presented a reduced miR-192-5p activity (Supplementary Fig. S4A and S4B). In HLF cells, infection with lentivirus pmir-192 significantly increased the expression level and activity

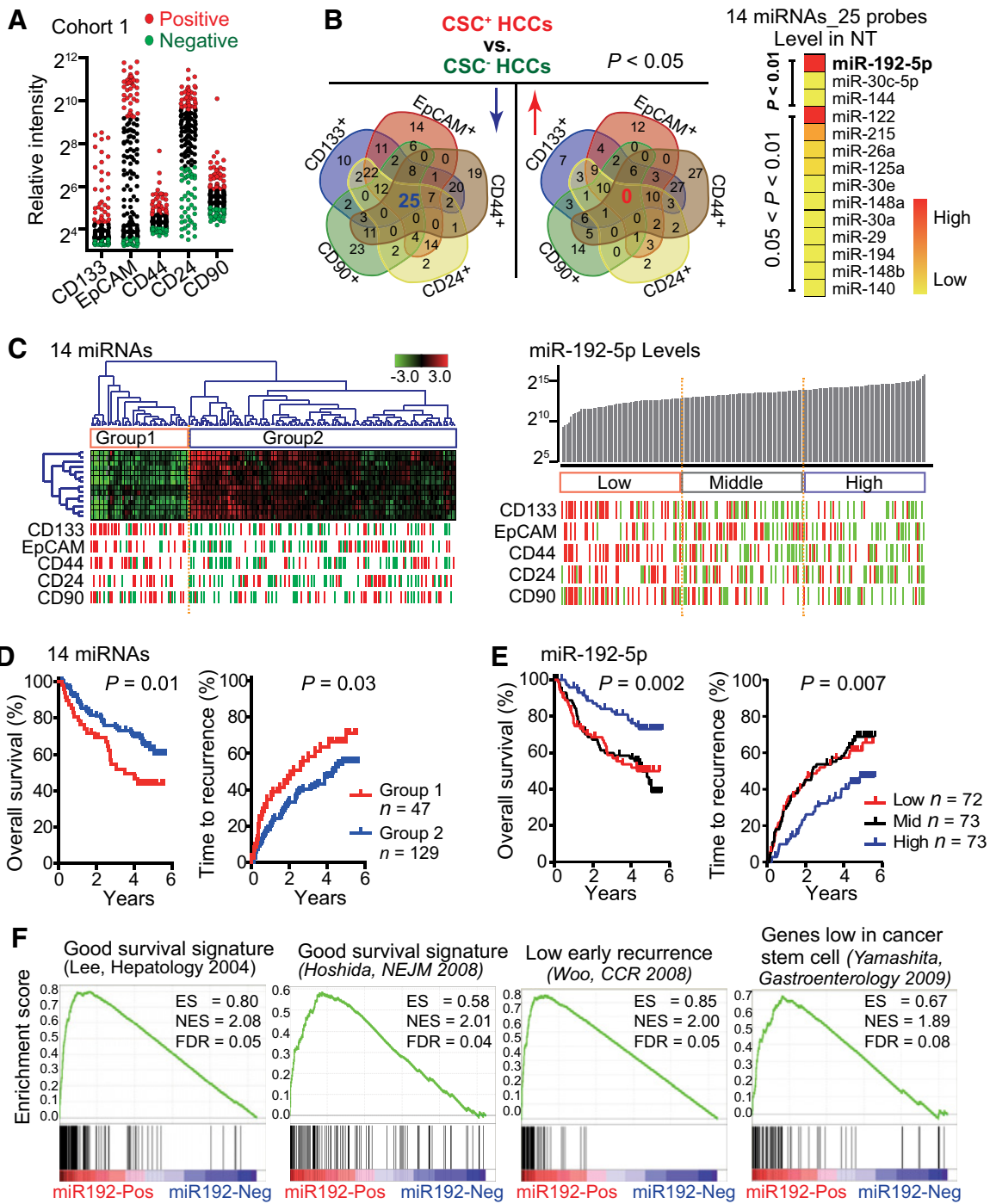
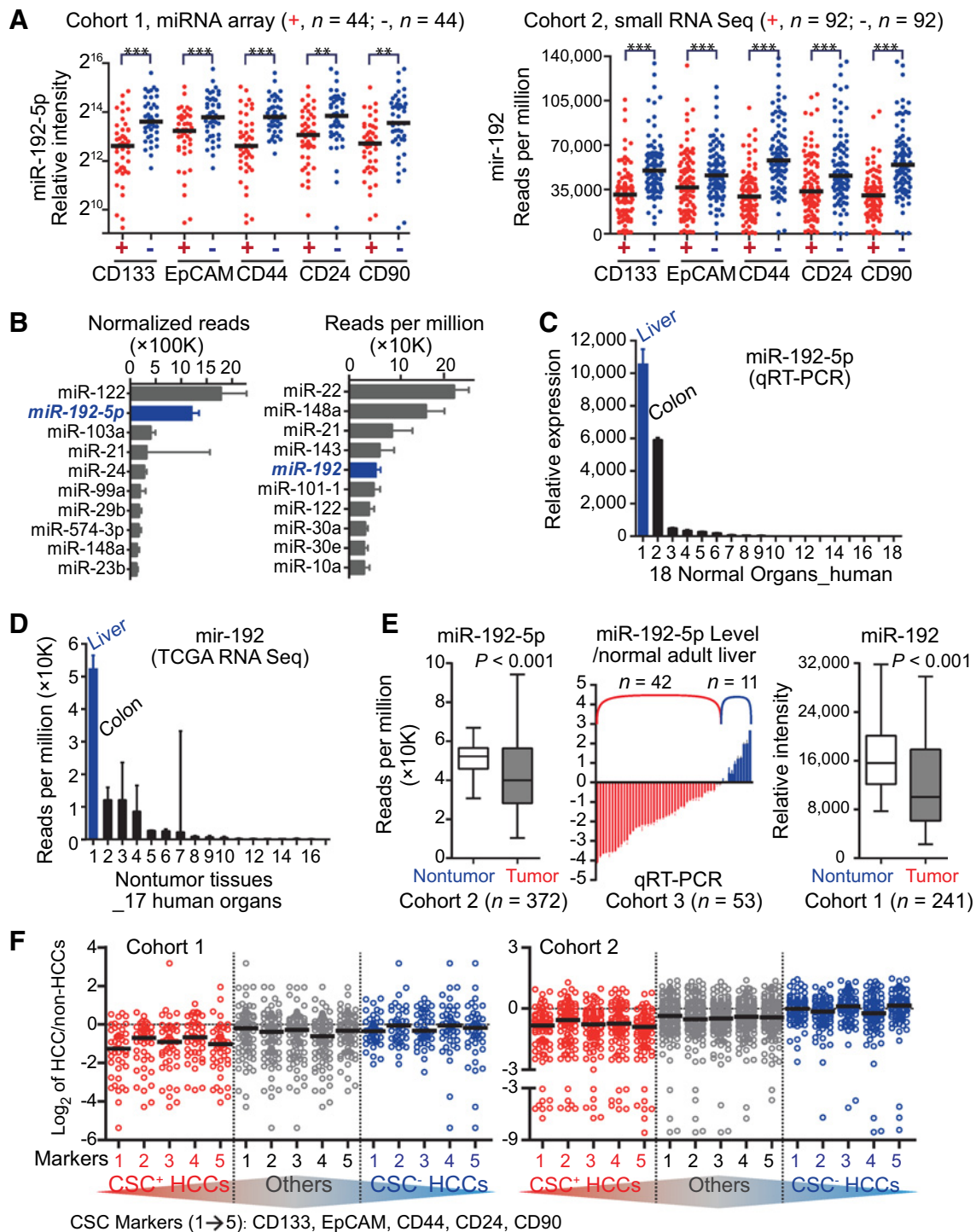


Figure 1.

A group of miRNAs were significantly downregulated in five different groups of CSC⁺ HCCs in Cohort 1, and the top one was miR-192-5p. **A**, Relative levels of five different hepatic CSC biomarkers. For each biomarker, red and green dots refer to patients with HCC with the top 25% expression levels (CSC⁺ HCCs) and patients with the bottom 25% levels (CSC⁻ HCCs), respectively. **B**, Venn Diagram analysis of miRNAs that were significantly ($P < 0.05$) altered in CSC⁺ HCCs versus CSC⁻ HCCs for each CSC biomarker. The abundance of 14 miRNAs (representing 25 miRNA probes) in nontumor tissues from patients with HCC is shown in the heat map. **C**, Hierarchical clustering analysis of 14 miRNAs revealed two different groups. The relative intensity of miR-192-5p in tumor was ranked. The positive (red bar) and negative (green bar) statuses of five CSC biomarkers are labeled correspondingly for each case. **D**, Kaplan-Meier curves of overall survival and time to recurrence of two identified HCC groups by 14 CSC miRNAs. **E**, Kaplan-Meier curves of overall survival and time to recurrence according to miR-192-5p levels (tertile division). **F**, GSEA analysis was performed to identify functionally related "gene sets" with statistically significant enrichment, using miR-192-5p-related genes identified from Cohort 1.

**Figure 2.**

miR-192-5p was a liver-abundant and -specific miRNA, and was significantly reduced in tumors compared with nontumors from patients with CSC⁺ HCC. **A**, Expression levels of mature miR-192-5p and miR-192 precursor in five groups of CSC⁺ HCCs and CSC⁻ HCCs from miRNA array data of HCC Cohort 1 (left) and Cohort 2 (right). The unpaired t test was used for Cohort 1, and nonparametric test was used for Cohort 2. **, $P < 0.01$; ***, $P < 0.001$. **B**, Reads distribution of the top 10 most abundant mature miRNAs in human hepatocytes (left) and the top 10 most abundant miRNA precursors in human nontumor liver tissues from HCC Cohort 2 (right). **C**, miR-192-5p expression was examined in 18 normal adult organs via qRT-PCR. From 1 to 18, they are liver, colon, brain, small intestine, kidney, testis, cerebellum, bone marrow, spinal cord, thymus, spleen, lung, skeletal muscle, salivary gland, placenta, prostate, adrenal gland, and uterus. **D**, The level of miR-192 is shown in nontumor tissues from 17 human organs in TCGA database. From 1 to 17, they are liver, colon, esophagus, kidney, rectum, pancreas, stomach, thyroid, thymus, skin, endometrium, lung, head and neck, prostate, cervix, breast, and bladder. **E**, The relative level of mature miR-192-5p and precursor miR-192 in tumor tissues and nontumor tissues from HCC cohorts 1–3. Paired t test (Cohort 1) and nonparametric t test (Cohort 2) were used. **F**, The log₂ ratio (tumor vs. nontumor) of miR-192-5p and miR-192 in different groups of CSC⁺ HCCs, CSC⁻ HCCs, and other HCCs from HCC cohorts 1–2.

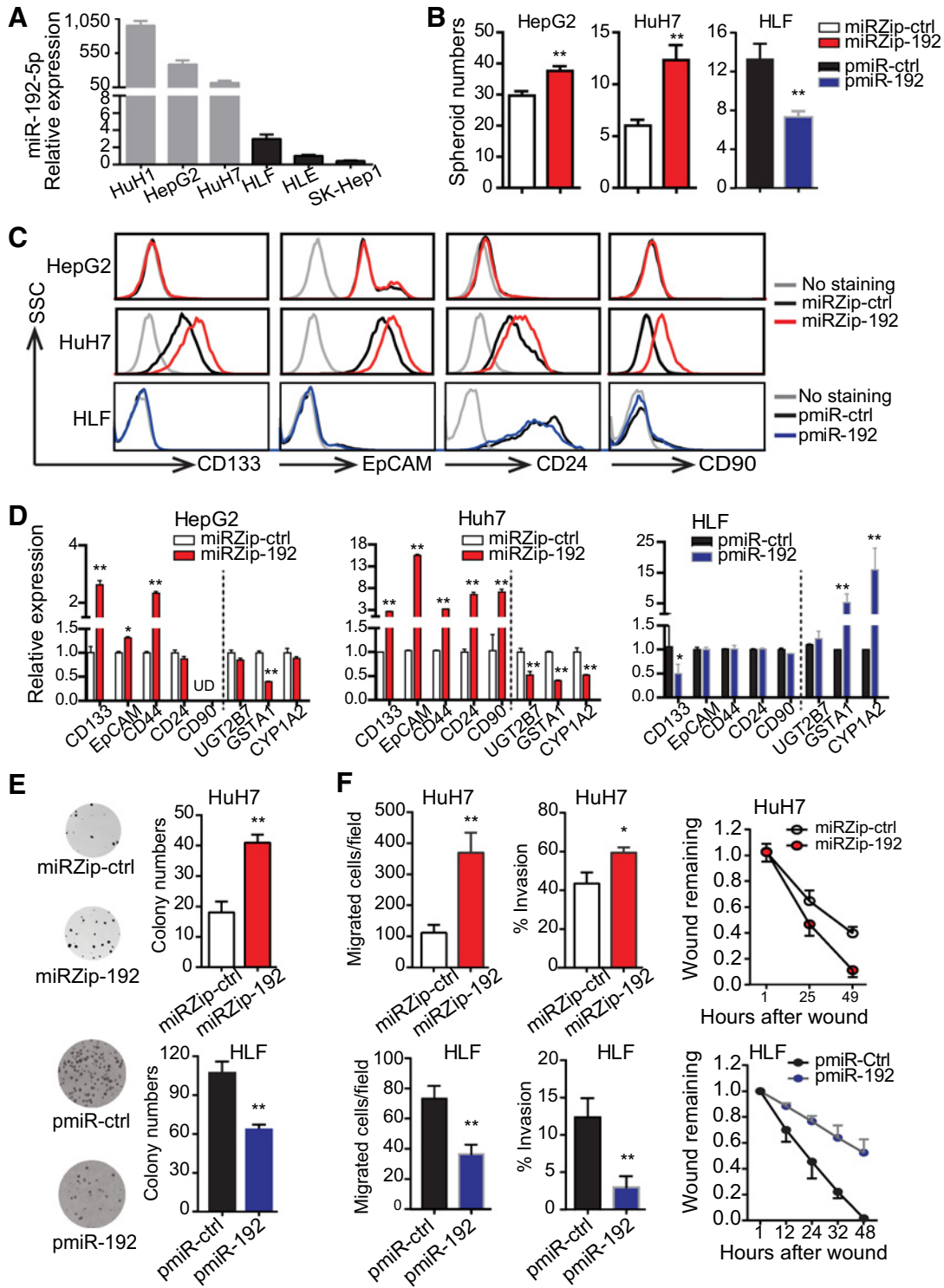


Figure 3. miR-192-5p suppressed the CSC features in HCC cells. **A**, The relative level of miR-192-5p in six HCC cell lines. **B** and **C**, Spheroid formation assay (**B**) and FACS analysis (**C**) in an ultralow-attachment plate were performed using HepG2 and HuH7 cells infected with lentivirus miRZip-ctrl or miRZip-192 and using HLF cells infected with lentivirus pmiR-ctrl or pmiR-192. For FACS analysis, APC-conjugated antibodies were used. **D**, Expression of a group of genes was examined in HepG2 and HuH7 cells infected with lentivirus miRZip-ctrl or miRZip-192, as well as in HLF cells infected with lentivirus pmiR-ctrl or pmiR-192. UD, under-detected. **E**, Colony formation was performed using HuH7 cells infected with lentivirus miRZip-ctrl or miRZip-192 and using HLF cells infected with lentivirus pmiR-ctrl or pmiR-192. The representative dishes are shown in the left plot. **F**, The migration/invasion assay was performed using HuH7 cells and HLF cells with altered miR-192-5p. For wound-healing assay, scratches were generated in confluent monolayer cells, and the degree of "wound remaining" was measured. The Student *t* test was used in **B**, **D** and **E**, and for migration/invasion assay in **F**. *, $P < 0.05$; **, $P < 0.01$.

of miR-192-5p, as shown by qRT-PCR and luciferase assay (Supplementary Fig. S4C).

In HuH7 and HepG2 cells, suppressing miR-192-5p by miRZip-192 significantly increased their spheroid formation (Fig. 3B), and CSC populations with different biomarkers, i.e., EpCAM⁺ populations in both cell lines, as well as CD133⁺, CD24⁺, and CD90⁺ populations in HuH7 cells (Fig. 3C). Suppressing miR-192-5p also increased CSC-biomarker expression, reduced levels of hepatocyte metabolism-related genes, and increased pluripotency marker expression (Fig. 3D; Supplementary Fig. S4D). In contrast, forced expression of miR-192-5p inhibited the stemness features of HLF cells, as shown by significantly reduced spheroid formation, reduced CD24⁺ CSC populations, decreased expression of several CSC biomarkers, and increased expression of genes related to functional metabolism in hepatocytes (Fig. 3B–D).

Previously, miR-192-5p was reported to promote cell proliferation and have a controversial role in regulating cell metastasis in HCC cell lines (35, 36). Thus, we examined these roles of miR-192-5p in HLF and HuH7. We found that miR-192-5p played a suppressive role in HCC colony formation, a cell tumorigenic feature (Fig. 3D), and cell migration and invasion, cell-invasive features (Fig. 3E and F; Supplementary Fig. S4F and S4G). Consistent with this observation, we noticed that forced expression of

miR-192-5p delayed tumor onset and reduced the tumor size in tumorigenicity assay (Supplementary Fig. S5A). These observations were consistent with the role of miR-192-5p in suppressing CSC features. However, in HLF and HuH7 cells, miR-192-5p did not appear to regulate cell proliferation markedly (Supplementary Fig. S5B).

Furthermore, Ingenuity Pathway Analysis using miR-192-5p-related genes identified in Cohort 1 revealed that genes positively related to miR-192-5p were involved in normal metabolic functions of differentiated hepatocytes, whereas genes negatively related to miR-192-5p were associated with increased cell invasion (Supplementary Fig. S1E). Collectively, these results demonstrate that miR-192-5p functionally suppresses CSC-related malignant features of HCC.

Roles of miR-192-5p in suppressing CSC-related features were partially through targeting PABPC4

To investigate the mechanism of miR-192-5p in suppressing hepatic CSC-related features, proteomics analysis using HLF cells was performed to screen for key targets of miR-192-5p. A total of 2,746 proteins were identified, and 123 proteins were significantly downregulated by miR-192-5p overexpression (Fig. 4A). Among them, ALCAM, PABPC4, and PRKAR1A were predicted targets of

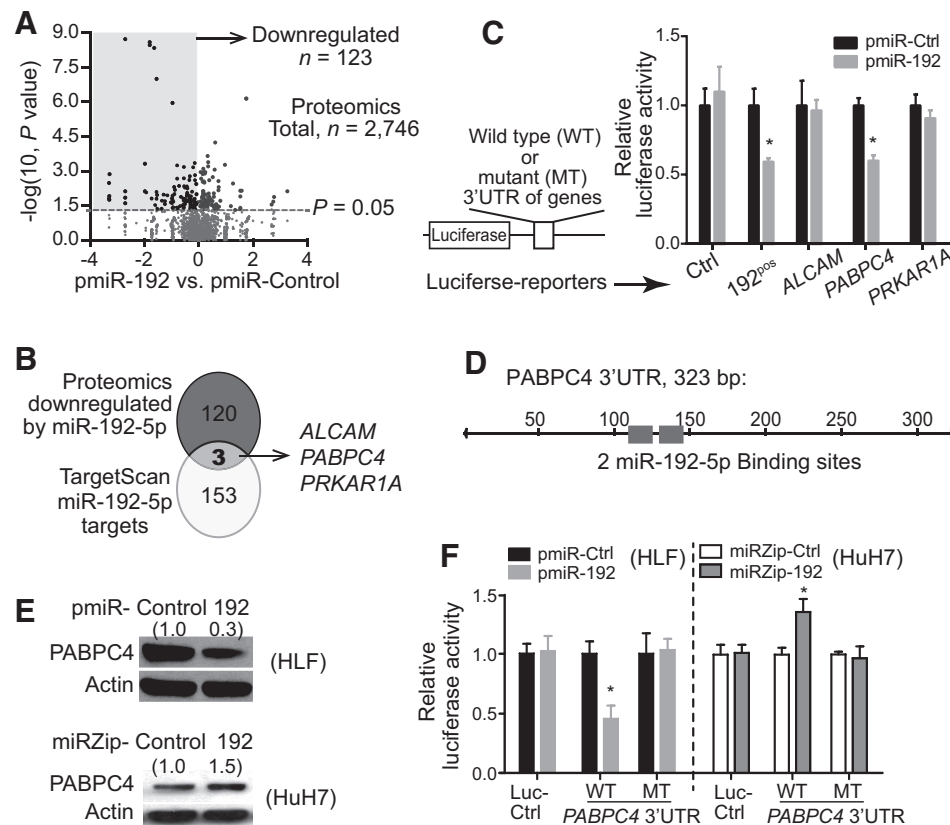


Figure 4.

PABPC4 was the direct target of miR-192-5p. **A**, Scatter plot of the fold changes for the identified proteins from Proteomics analysis. **B**, Venn diagram analysis of predicted targets from TargetScan and proteins being downregulated by miR-192-5p. **C**, Luciferase activities were measured using reporters with WT miR-192-5p-binding sites in the 3'-UTR of luciferase vector. Luc-192^{pos} was used as the positive control. **D**, Predicted miR-192-5p-binding sites in 3'-UTR sequences of human PABPC4. **E**, The expression level of PABPC4 in HLF cells infected with lentivirus pmiR-192 and in HuH7 cells infected with lentivirus miRZip-192 as determined by Western blotting. **F**, Luciferase activities of reporter plasmids with WT or MT PABPC4 in HLF cells and HuH7 cells. *, $P < 0.05$.

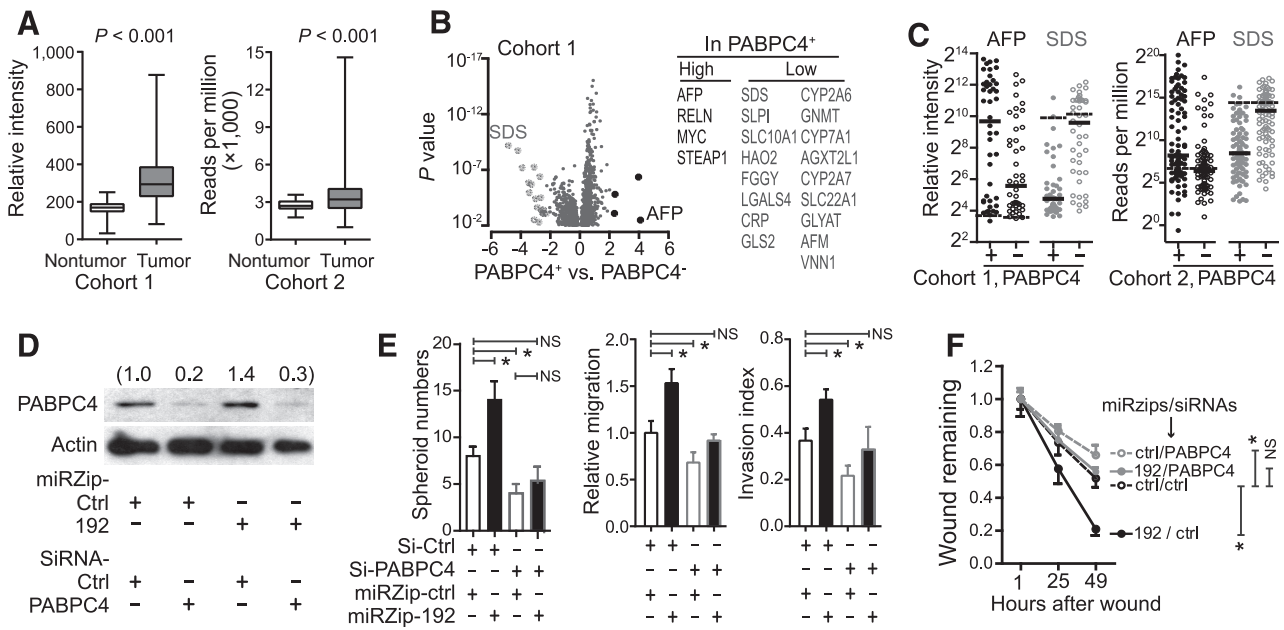


Figure 5. PABPC4 was the key downstream target of miR-192-5p to regulate HCC-malignant features. **A**, PABPC4 expression in tumor tissues compared with nontumor tissues from patients with HCC in Cohort 1 (176 HCC cases with paired tumor and nontumor) and Cohort 2 (50 nontumor liver tissues and 367 HCCs). **B**, Scatter plots of genes that were significantly altered ($P < 0.01$) in PABPC4⁺ HCCs compared with PABPC4⁻ HCCs. **C**, The relative levels of AFP and SDS in PABPC4⁺ HCCs and PABPC4⁻ HCCs in two cohorts. **D-F**, Western blot of PABPC4 (**D**), spheroid assay, cell migration, and cell invasion assay (**E**), as well as wound-healing assay (**F**) were performed in HuH7 cells infected with lentivirus miRZip-ctrl or miRZip-192, followed with transfection with siRNA-control or siRNA-PABPC4. *, $P < 0.05$; NS, nonsignificant.

miR-192-5p in TargetScan (Fig. 4B). In 293T cells, ALCAM was reported to be the direct target of miR-192-5p (37). Thus, the miR-192-5p-binding regions of the 3'-untranslated regions (UTR) for these three genes were inserted to 3'-UTR of the luciferase reporter. The dual-luciferase assay in HLF cells showed that PABPC4 was significantly suppressed after miR-192-5p overexpression, whereas ALCAM and PRKAR1A were not (Fig. 4C).

The 3'-UTR of PABPC4 contains two miR-192-5p-binding sites (Fig. 4D). As shown in Fig. 4E, suppressing miR-192-5p significantly increased the protein level of PABPC4 in HuH7 cells, whereas miR-192-5p overexpression significantly suppressed PABPC4 in HLF cells. Furthermore, when two wild-type miR-192-5p-binding sequences in the 3'-UTR of PABPC4 were present, forced expression of miR-192-5p decreased the luciferase activity, whereas suppressed miR-192-5p increased the luciferase activity. This effect was significantly canceled when the partial corresponding miR-192-5p-binding sites were mutated (Fig. 4F). These demonstrate that miR-192-5p targets PABPC4 via the binding of miR-192-5p to the 3'-UTR of PABPC4.

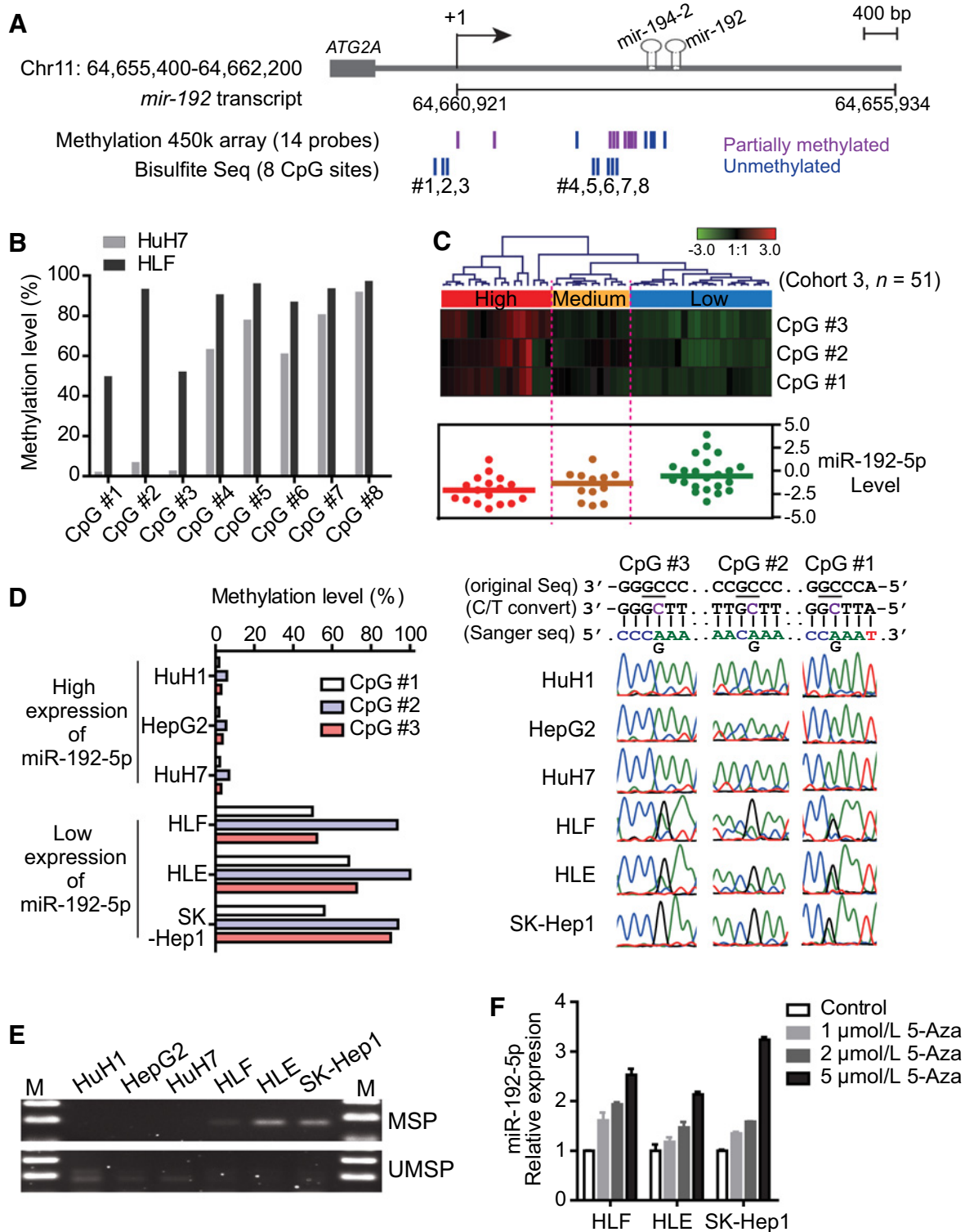
PABPC4, a Poly (A)-binding protein, is expressed at a higher level in colon cancer and lung adenocarcinoma compared with nontumor tissues (38, 39). However, the expression and role of PABPC4 in HCC remain unknown. As shown in Fig. 5A, PABPC4 was significantly upregulated in tumor tissues compared with nontumor tissues in both cohorts. In addition, we divided 176 patients with HCC in Cohort 1 into 4 groups based on PABPC4 expression level followed by gene expression profile comparison between HCC cases with the top quartile expression of PABPC4 (PABPC4⁺ HCCs) and those with the bottom quartile level of PABPC4 (PABPC4⁻ HCCs). A total of 985 genes showed significantly higher levels in PABPC4⁺ HCCs ($P < 0.01$), with four

genes, including AFP and MYC, having ≥ 5 -fold increased expression. The expression of 437 genes was significantly reduced in PABPC4⁺ HCCs. Seventeen genes had a lower than 0.2-fold decreasing, among which, 14 genes were clearly related to hepatic metabolic functions, including SDS, SLC10A1, and a group of CYPs (Fig. 5B). Figure 5C shows a significant higher AFP level and a significant lower SDS level in PABPC4⁺ HCCs compared with PABPC4⁻ HCCs in both cohorts. These results indicate that the abnormally highly expressed PABPC4 in HCCs might play important roles in increasing CSC-related malignant features.

We used siRNA against PABPC4 to reduce the expression of PABPC4 (Supplementary Fig. S5C). In HuH7 cells infected with miRZip-192, PABPC4 siRNA diminished the increased level of PABPC4 compared with control siRNA (Fig. 5D) and significantly reduced the spheroid formation (Fig. 5E, left). The number of formed spheroids was similar between control cells and cells with suppressed miR-192-5p and silenced PABPC4. These results indicate that silencing PABPC4 could ease the induced spheroid formation caused by suppressing miR-192-5p. Consistent data were obtained from the cell migration and cell invasion assays (Fig. 5E) and wound-healing assays (Fig. 5F). Similar migration and invasion rates were observed in both control cells and cells with suppressed miR-192-5p and silenced PABPC4. Taken together, the roles of miR-192-5p in suppressing CSC-related features were mediated by targeting PABPC4.

HCCs with a low level of miR-192-5p harbored a miR-192 hypermethylated promoter

Due to the reduced level of mature miR-192-5p and its precursor in HCCs, especially in CSC⁺ HCCs, the genetic alterations of the miR-192 gene were examined on its copy-number alteration

**Figure 6.**

The reduced level of miR-192-5p in HCCs was related to a hypermethylated mir-192 promoter. **A**, The schematic genomic structure of the primary mir-192 transcript, and locations of both 8 CpG sites and 14 methylation detection probes from UCSC database. The methylation status in hepatocytes is labeled. **B**, Methylation levels of 8 CpG sites by the pyrosequencing method in HLF and HuH7 cells. **C**, Hierarchical clustering of the methylation values of CpG sites #1, #2, and #3 in Cohort 3. Three groups were identified, i.e., high-, medium-, and low-methylation groups. In each group, the miR-192-5p expression level is shown. **D**, Methylation levels of CpG sites #1, #2, and #3 in 6 HCC cell lines with different expression levels of miR-192-5p by pyrosequencing (left) and Sanger sequencing (right). **E**, Methylation-specific PCR and unmethylation-specific PCR were performed using MSPs and UMSPs in 6 HCC cell lines with their bisulfite-converted DNAs as templates. **F**, miR-192-5p expression level in three HCC cell lines treated with different dose of 5-AZA for 3 days.

as well as methylation status. In an array-based comparative genomic hybridization dataset of 76 HCCs (GSE14322; ref. 6), there was no observed DNA deletion of mir-192. In the University of California Santa Cruz (UCSC) genome browser, Bisulfite Sequencing data revealed eight CpG sites in the mir-192 promoter region. These CpG sites were unmethylated in liver-related tissues such as hepatocytes and HepG2 cells, but highly methylated in cells from many other tissues (Supplementary Fig. S6A; Fig. 6A). We thus performed pyrosequencing on bisulfite-converted DNA to investigate these eight suggested CpG sites in cells with high (HuH7) and low (HLF) miR-192-5p expression levels. As shown in Fig. 6B, the methylation levels on the first three CpGs were 13- to 22-folds lower in HuH7 compared with HLF. Subsequently, methylation of these three CpG sites was explored in 51 HCC cases from Cohort 3. As shown in Fig. 6C, mir-192 promoter methylation level ranged between 0.4% and 43.5% and inversely correlated with miR-192-5p expression level.

Consistent data were also obtained in HCC cell lines (Fig. 6D). Pyrosequencing data revealed a hypermethylation status of three CpG sites in three HCC cell lines with low levels of miR-192-5p, i.e., HLF, HLE, and SK-Hep1 cells, whereas a low methylation status in cells with high levels of miR-192-5p, i.e., HuH1, HepG2, and HuH7. We further applied Sanger Sequencing with the bisulfite-treated DNA as the template to validate methylation status of three CpG sites in these six cell lines. Consistent with Pyrosequencing data, unmethylated CpG sites #1, #2, and #3 were observed in HuH1, HepG2, and HuH7 cells, whereas methylated sites were detected in HLF, HLE, and SK-Hep1 cells (Fig. 6D). Methylation-specific PCR and unmethylation specific PCR also showed consistent results (Fig. 6E). In addition, 5-AZA significantly induced the expression of miR-192-5p in a dose-dependent manner in HLF, HLE, and SK-Hep1 cells with hypermethylated mir-192 promoters (Fig. 6F).

Both *TP53* mutation and hypermethylation of mir-192 in HCCs impeded the transcriptional activation of miR-192-5p by p53

In multiple myeloma and HCC, p53 induces mir-192 expression (40, 41). The p53-binding sites have been identified in mir-192 promoter region (40). Our in-depth analysis shows that the identified CpG sites #2 and #3 sit within the p53-binding sites (20 bp) of mir-192 promoter (Fig. 7A). *TP53* mutations are the most frequent events in HCCs compared with other genes (42, 43). Approximately 30% of HCC tumors contained a *TP53* mutation with most mutations occurring in the p53 DNA-binding domain. R249S was the most frequent one. Thus, we reasoned that mir-192 promoter hypermethylation and *TP53* mutations might jointly contribute to the silencing of miR-192-5p in CSC⁺ HCCs.

In order to test this hypothesis, we constructed two nucleotide fragments, i.e., unmethylated mir-192 promoter region with luciferase gene and methylated mir-192 promoter with luciferase (Fig. 7A). In the presence of the unmethylated mir-192 promoter, p53 significantly induced mir-192 promoter activity (HLF, 43-fold; HuH7, 50-fold), whereas mutant p53/R249S did not induce mir-192 promoter activity at all (Fig. 7B). In addition, in the presence of methylated mir-192 promoter, wild-type p53 induced mir-192 promoter activity by 11-fold in HLF and 27-fold in HuH7, whereas mutant p53/R249S did not induce or even reduced the mir-192 promoter activity (HLF, 0.74-fold; HuH7, 0.67-fold). Comparably, the p53-induced promoter activity was 2 to 4 times higher for the unmethylated mir-192 promoter than that for the methylated one. The mutant p53/R249S did not induce either methylated or

unmethylated mir-192 promoter activity, but reduced the methylated mir-192 promoter activity compared with the unmethylated one. Thus, two levels of DNA alterations in HCC, including *TP53* mutations and hypermethylation of mir-192, impeded the binding of p53 as the transcriptional factor to mir-192 promoter, which led to the reduced transcriptional induction of mir-192.

We then explored the relationship of *TP53* mutations, mir-192 promoter methylation, and mir-192 expression in patients with HCC from Cohort 2. With the ranking of mir-192 level in 286 HCCs from high to low, the methylation level of mir-192 promoter was gradually increased as represented by the beta-values of 14 methylation probes (Fig. 7C). *TP53* mutation data were available in 242 of the 286 HCCs. Consistent with the published data, 33.5% cases (81 of 242) harbored a *TP53* mutation, and R249S was the most frequent one (9 of 81). Figure 7D showed that the level of mir-192 was highest in HCC cases with a wild-type p53 and low methylation level of mir-192 promoter, and lowest in HCC cases with a mutant p53 and high-methylation level of mir-192 promoter. These findings consistently indicate that the low miR-192-5p level in HCC cases was related to the hypermethylation of the mir-192 promoter as well as *TP53* mutations.

Among the five groups of CSC⁺ HCC cases with significant low levels of miR-192-5p in Cohort 2, higher *TP53* mutation rates presented in four groups, significant higher methylation levels of mir-192 promoter were in all five groups, and significant higher PABPC4 reads exhibited in four groups compared with those in the corresponding CSC⁻ HCCs (Fig. 7E). Consistently, *TP53* mutation frequency and PABPC4 reads were also much higher in CSC⁺ HCC groups than those in CSC⁻ HCCs in Cohort 1 (Supplementary Fig. S6B). Therefore, in malignant HCC cases expressing high levels of CSC biomarkers, both *TP53* mutations and mir-192 promoter hypermethylation likely silenced the expression of miR-192-5p, which ensured an accumulation of PABPC4 eventually contributing to the CSC features in HCC (Fig. 7F).

Discussion

As a malignancy with an overall 5-year survival of less than 10%, HCC has received increasing attention from clinicians and researchers. Identification and functional characterization of hepatic CSCs have paved the way for HCC diagnosis and prognosis prediction as well as the development of potential novel HCC therapeutic strategies. Although a group of relevant hepatic CSC biomarkers have been identified, little is known about the implication of CSC heterogeneity and presence of shared molecular networks or even the genetic selective pressures.

From a large-scale cohort study, we identified a 14-miRNA signature shared by five different groups of patients with CSC⁺ HCC, who represent diverse HCC populations. Low levels of these miRNAs were associated with poor prognosis. These highlighted the important roles of the shared molecular events in regulating malignant features of HCC. In addition, the disparity of these different CSC populations has also been shown by miRNAs unique to each of the CSC⁺ HCC groups. Future investigations of these miRNAs may help to determine whether some of these different CSC populations are lineage-restricted.

MiR-192-5p was the top CSC-related miRNA and presented low levels in five different groups of patients with CSC⁺ HCC. The presented data demonstrate that this molecule holds a key role in suppressing hepatic tumorigenesis features. (1) miR-192-5p was

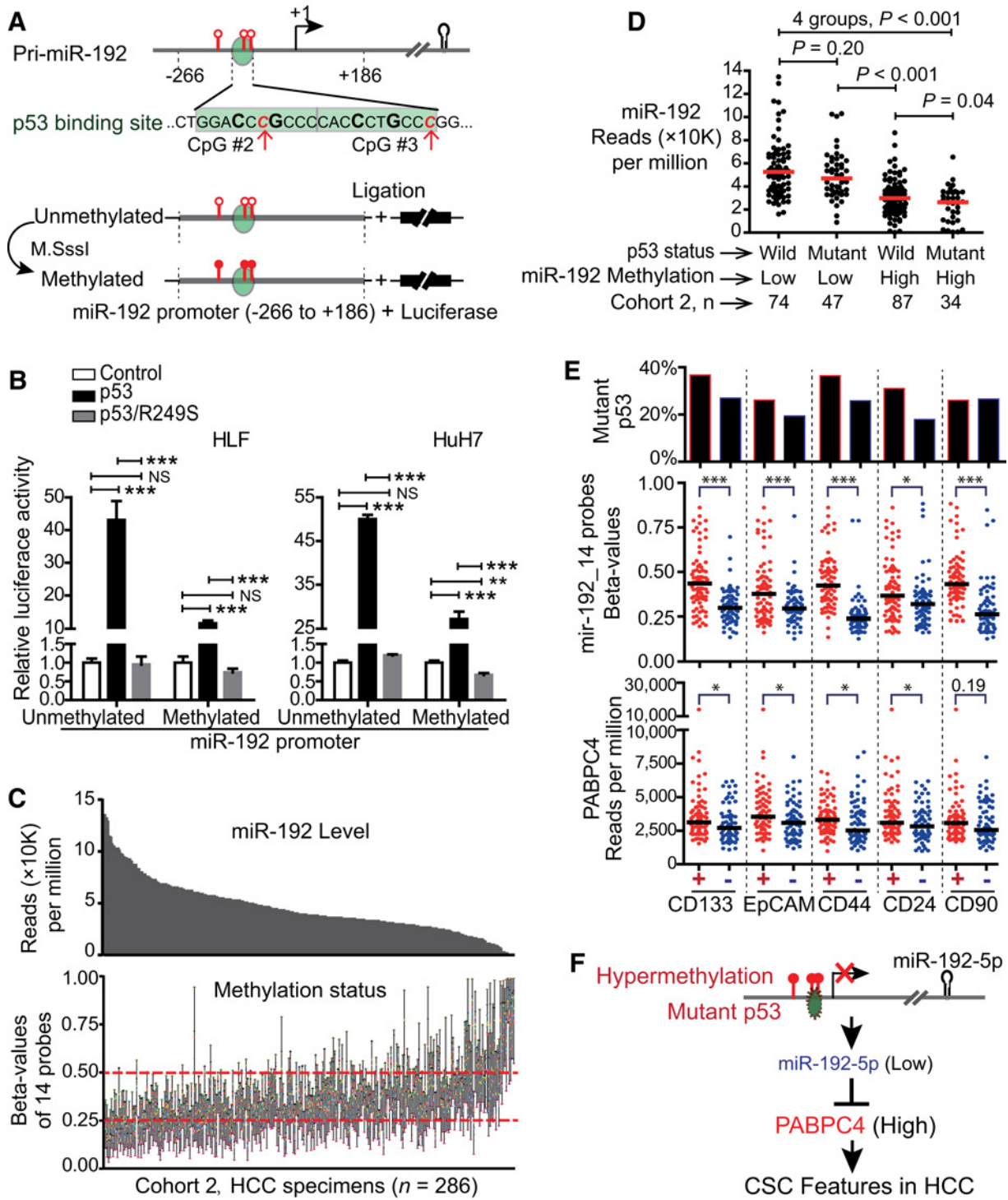


Figure 7. TP53 mutations and the miR-192 promoter hypermethylation in HCCs blocked the transcriptional activation of miR-192-5p, especially in CSC⁺ HCCs. **A**, Schematic genomic structures of the miR-192 promoter region and the reporter construction of the methylated and unmethylated miR-192 promoters. Two p53-binding sites overlap with CpG sites #2 and #3. **B**, The dual-luciferase assay was performed in HLF and HuH7 cells. Cells were cotransfected with the methylated/unmethylated miR-192 promoter, pRL-CMV, and pXF6F (control) or pXF6F-p53 (wild-type p53) or pXF6F-p53-R249S (mutant p53 R249S). **C**, Expression of *mir-192* precursor (top) is shown for each HCC individual in cohort 2, in which DNA methylation status was represented by 14 methylation probes (bottom). The black vertical lines depict the range of β values of 14 probes. **D**, The relative level of miR-192 in HCC cases with available methylation 450K array data and known TP53 mutation status ($n = 242$; Cohort 2). **E**, The frequency of TP53 mutation (top), mean β values of 14 miR-192 methylation probes (middle), and PABPC4 expression level (bottom) in five groups of CSC⁺ HCCs and CSC⁻ HCCs of Cohort 2. Nonparametric Mann-Whitney rank test was performed. **F**, The schematic model of the miR-192-5p regulatory pathway for amending hepatic CSC features. ***, $P < 0.001$; NS, nonsignificant.

liver-abundant and liver-specific, as well as significantly down-regulated in HCCs, especially in CSC⁺ HCCs. (2) Both genetic (*TP53* mutation) and epigenetic (miR-192 promoter hypermethylation) alterations significantly contributed to the reduced level of miR-192-5p in multiple groups of CSC⁺ HCCs. (3) HCCs with a reduced level of miR-192-5p had shorter overall survival and time to recurrence at a dose-dependent manner in two different HCC cohorts (Cohort 1 and Cohort 3). Lian and colleagues had also reported that the reduced level of miR-192 was associated with poor overall survival (35). (4) miR-192-5p functionally reduced the CSC populations and suppressed CSC features in HCC cell lines. In addition, several groups have also reported the roles of miR-192-5p in suppressing tumor progression of myeloma, ovarian cancer, and pancreatic cancer (40, 44, 45). In colon cancer, the oncogenic PI3K/Akt pathway suppressed miR-192-5p expression (46), which was also confirmed in our HCC cell lines (Supplementary Fig. S6C–S6E). miR-192-5p level is elevated in serum from patients with HCC compared with healthy controls (47, 48), but it remains unknown whether miR-192-5p is actively or passively secreted into circulation or what is the role of miR-192-5p in our circulating system. Consistent with our findings, one study identified miR-192-5p as one of the miRNAs in HCC cells that regulate cell migration and cell invasion (35). Together, for HCCs expressing high level of CSC biomarkers or low level of miR-192-5p, delivering miR-192-5p to the liver may be a potent strategy for HCC therapy. Such a strategy has less toxicity to the liver due to the abundance of miR-192-5p in liver and its capacity to inhibit hepatic CSC features. We will further systemically test this possibility in future.

Mutations in the *TP53* gene are considered to be cancer drivers for HCC development and early events in the hepatic carcinogenesis process (16, 29, 42). In this vein, miR-192-5p down-regulation might also be an early event in HCC to allow liver cells to obtain CSC features and contribute to tumor initiation. It remains unknown whether the methylation of miR-192 promoter is also an early event in HCC development and when it occurs. Further studies on *TP53* mutations and the methylation/expression of miR-192-5p in cirrhotic livers as well as inflammatory livers will help to answer these questions.

Our study focused on the five CSC biomarkers confirmed in primary HCCs to identify CSC⁺ HCC cases for all of these described analysis. In HCC cell lines, there are other CSC biomarkers for enriching hepatic CSCs, such as OV6, CK19, DCLK1, etc. (17, 18, 49). Our data revealed that miR-192-5p expressed at a significant low level in OV6⁺, CK19⁺, and DCLK1⁺HCCs. Ma and colleagues reported that the combination of CD133 and ALDH defined hepatic CSCs more accurately, shown by an ascending tumorigenic potential in the order of CD133⁺ALDH⁺ HCC cells > CD133⁺ALDH⁻ > CD133⁻ALDH⁻ (50). Consistently, our data displayed a high level of miR-192-5p in CD133⁻ALDH1A1⁻ HCCs (Supplementary Fig. S3C and S3D). However, miR-192-5p expressed at a significantly higher level in ALDH1A1⁺ HCCs

compared with its level in ALDH1A1⁻ HCCs. It might be worth to explore whether ALDH1A1 alone could act as a hepatic CSC marker, as well as the relationship of miR-192-5p with ALDH1A1. Global analysis of primary HCC cells as well as HCC cell lines using single-cell sequencing technology may serve as a better method to unbiasedly identify all CSC populations in patients with HCC and provide a precise resolution of their shared and unique features in the context of tumor microenvironment.

In summary, our study has revealed a shared genetic regulatory signaling pathway (miR-192 promoter hypermethylation/*TP53* mutation/reduced miR-192-5p/increased PABPC4) in five different groups of CSC⁺ HCCs. Due to the nature of *TP53* mutation as an early event in HCC, the activation of this pathway may allow a subpopulation of hepatocytes to obtain the tumor initiation ability, leading to HCC development. These findings improved our understanding on CSC heterogeneity and elucidated the potential role of miR-192-5p in early diagnosis and/or the molecular therapeutic target for patients with HCC.

Disclosure of Potential Conflicts of Interest

L.L. Wong reports receiving honoraria from the speakers' bureau of Eisai and Bayer. No potential conflicts of interest were disclosed by the other authors.

Authors' Contributions

Conception and design: X. Wei, X. Zheng, L. Jin, J. Ji

Development of methodology: Y. Gu, X. Wei, X. Zheng, J. Ji

Acquisition of data (provided animals, acquired and managed patients, provided facilities, etc.): Y. Gu, X. Wei, Y. Sun, H. Gao, L.L. Wong, L. Jin, B. Hernandez, K. Peplowska, X. Zhao, Z.-Y. Tang, J. Ji

Analysis and interpretation of data (e.g., statistical analysis, biostatistics, computational analysis): Y. Gu, X. Wei, Y. Sun, X. Zheng, L. Jin, K. Peplowska, J. Ji

Writing, review, and/or revision of the manuscript: X. Wei, Y. Sun, B. Hernandez, K. Peplowska, Q.-M. Zhan, X.-H. Feng, J. Ji

Administrative, technical, or material support (i.e., reporting or organizing data, constructing databases): Y. Gu, X. Wei, H. Gao, X. Zheng, B. Hernandez, X. Zhao, J. Ji

Study supervision: Z.-Y. Tang, J. Ji

Others (operated animal experiments): N. Liu

Acknowledgments

The authors thank Dr. Xin W. Wang from NCI in the United States for his critical reading and for sharing the information of *TP53* mutation in Cohort 1.

This work was supported by National Natural Science Foundation of China (No. 81672905 and 81874054, to J. Ji), the Fundamental Research Funds for the Central Universities in China (to J. Ji), and the Thousand Young Talents Plan of China (to J. Ji). The study was also supported in part by funds from NCI P30-CA071789 (H. Gao, L. Jin, L.L. Wong, B. Hernandez, and K. Peplowska).

The costs of publication of this article were defrayed in part by the payment of page charges. This article must therefore be hereby marked *advertisement* in accordance with 18 U.S.C. Section 1734 solely to indicate this fact.

Received June 1, 2018; revised October 11, 2018; accepted November 30, 2018; published first December 7, 2018.

References

1. Ferlay J, Soerjomataram I, Dikshit R, Eser S, Mathers C, Rebelo M, et al. Cancer incidence and mortality worldwide: sources, methods and major patterns in GLOBOCAN 2012. *Int J Cancer* 2015;136:E359–86.
2. Jemal A, Bray F, Center MM, Ferlay J, Ward E, Forman D. Global cancer statistics. *CA Cancer J Clin* 2011;61:69–90.
3. Llovet JM, Ricci S, Mazzaferro V, Hilgard P, Gane E, Blanc JF, et al. Sorafenib in advanced hepatocellular carcinoma. *N Engl J Med* 2008;359:378–90.
4. Knox JJ, Cleary SP, Dawson LA. Localized and systemic approaches to treating hepatocellular carcinoma. *J Clin Oncol* 2015;33:1835–44.
5. Gupta PB, Chaffer CL, Weinberg RA. Cancer stem cells: mirage or reality? *Nat Med* 2009;15:1010–2.

6. Oikawa T. Cancer stem cells and their cellular origins in primary liver and biliary tract cancers. *Hepatology* 2016;64:645–51.
7. Lee TK, Castilho A, Cheung VC, Tang KH, Ma S, Ng IO. CD24(+) liver tumor-initiating cells drive self-renewal and tumor initiation through STAT3-mediated NANOG regulation. *Cell Stem Cell* 2011;9:50–63.
8. Wan S, Zhao E, Kryczek I, Vatan L, Sadovskaya A, Ludema G, et al. Tumor-associated macrophages produce interleukin 6 and signal via STAT3 to promote expansion of human hepatocellular carcinoma stem cells. *Gastroenterology* 2014;147:1393–404.
9. Yamashita T, Ji J, Budhu A, Forgues M, Yang W, Wang HY, et al. EpCAM-positive hepatocellular carcinoma cells are tumor-initiating cells with stem/progenitor cell features. *Gastroenterology* 2009;136:1012–24.
10. Yang ZF, Ngai P, Ho DW, Yu WC, Ng MN, Lau CK, et al. Identification of local and circulating cancer stem cells in human liver cancer. *Hepatology* 2008;47:919–28.
11. Yang ZF, Ho DW, Ng MN, Lau CK, Yu WC, Ngai P, et al. Significance of CD90+ cancer stem cells in human liver cancer. *Cancer Cell* 2008;13:153–66.
12. Ma S, Tang KH, Chan YP, Lee TK, Kwan PS, Castilho A, et al. miR-130b Promotes CD133(+) liver tumor-initiating cell growth and self-renewal via tumor protein 53-induced nuclear protein 1. *Cell Stem Cell* 2010;7:694–707.
13. Ma S, Chan KW, Hu L, Lee TK, Wo JY, Ng IO, et al. Identification and characterization of tumorigenic liver cancer stem/progenitor cells. *Gastroenterology* 2007;132:2542–56.
14. Suetsugu A, Nagaki M, Aoki H, Motohashi T, Kunisada T, Moriwaki H. Characterization of CD133+ hepatocellular carcinoma cells as cancer stem/progenitor cells. *Biochem Biophys Res Commun* 2006;351:820–4.
15. Zhu Z, Hao X, Yan M, Yao M, Ge C, Gu J, et al. Cancer stem/progenitor cells are highly enriched in CD133+CD44+ population in hepatocellular carcinoma. *Int J Cancer* 2010;126:2067–78.
16. Tornesello ML, Buonaguro L, Tatangelo F, Botti G, Izzo F, Buonaguro FM. Mutations in TP53, CTNBN1 and PIK3CA genes in hepatocellular carcinoma associated with hepatitis B and hepatitis C virus infections. *Genomics* 2013;102:74–83.
17. Yamashita T, Wang XW. Cancer stem cells in the development of liver cancer. *J Clin Invest* 2013;123:1911–8.
18. Ji J, Wang XW. Clinical implications of cancer stem cell biology in hepatocellular carcinoma. *Semin Oncol* 2012;39:461–72.
19. Ji J, Yamashita T, Budhu A, Forgues M, Jia HL, Li C, et al. Identification of microRNA-181 by genome-wide screening as a critical player in EpCAM-positive hepatic cancer stem cells. *Hepatology* 2009;50:472–80.
20. Ji J, Yamashita T, Wang XW. Wnt/beta-catenin signaling activates microRNA-181 expression in hepatocellular carcinoma. *Cell Biosci* 2011;1:4.
21. Zhang J, Luo N, Luo Y, Peng Z, Zhang T, Li S. microRNA-150 inhibits human CD133-positive liver cancer stem cells through negative regulation of the transcription factor c-Myb. *Int J Oncol* 2012;40:747–56.
22. Ji J, Zheng X, Forgues M, Yamashita T, Wauthier EL, Reid LM, et al. Identification of microRNAs specific for epithelial cell adhesion molecule-positive tumor cells in hepatocellular carcinoma. *Hepatology* 2015;62:829–40.
23. Ji J, Wang XW. New kids on the block: diagnostic and prognostic microRNAs in hepatocellular carcinoma. *Cancer Biol Thera* 2009;8:1686–93.
24. Lee RC, Ambros V. An extensive class of small RNAs in *Caenorhabditis elegans*. *Science (New York, N.Y.)* 2001;294:862–4.
25. Kota J, Chivukula RR, O'Donnell KA, Wentzel EA, Montgomery CL, Hwang HW, et al. Therapeutic microRNA delivery suppresses tumorigenesis in a murine liver cancer model. *Cell* 2009;137:1005–17.
26. Budhu A, Jia HL, Forgues M, Liu CG, Goldstein D, Lam A, et al. Identification of metastasis-related microRNAs in hepatocellular carcinoma. *Hepatology* 2008;47:897–907.
27. Roessler S, Long EL, Budhu A, Chen Y, Zhao X, Ji J, et al. Integrative genomic identification of genes on 8p associated with hepatocellular carcinoma progression and patient survival. *Gastroenterology* 2012;142:957–66 e12.
28. Roessler S, Jia HL, Budhu A, Forgues M, Ye QH, Lee JS, et al. A unique metastasis gene signature enables prediction of tumor relapse in early-stage hepatocellular carcinoma patients. *Cancer Res* 2010;70:10202–12.
29. Woo HG, Wang XW, Budhu A, Kim YH, Kwon SM, Tang ZY, et al. Association of TP53 mutations with stem cell-like gene expression and survival of patients with hepatocellular carcinoma. *Gastroenterology* 2011;140:1063–70.
30. Kwee SA, Hernandez B, Chan O, Wong L. Choline kinase alpha and hexokinase-2 protein expression in hepatocellular carcinoma: association with survival. *PLoS One* 2012;7:e46591.
31. Ji J, Shi J, Budhu A, Yu Z, Forgues M, Roessler S, et al. MicroRNA expression, survival, and response to interferon in liver cancer. *N Engl J Med* 2009;361:1437–47.
32. Tabb DL. What's driving false discovery rates? *J Proteome Res* 2008;7:45–6.
33. Ji J, Zhao L, Budhu A, Forgues M, Jia HL, Qin LX, et al. Let-7g targets collagen type I alpha2 and inhibits cell migration in hepatocellular carcinoma. *J Hepatol* 2010;52:690–7.
34. Kakehashi A, Ishii N, Sugihara E, Gi M, Saya H, Wanibuchi H. CD44 variant 9 is a potential biomarker of tumor initiating cells predicting survival outcome in hepatitis C virus-positive patients with resected hepatocellular carcinoma. *Cancer Sci* 2016;107:609–18.
35. Lian J, Jing Y, Dong Q, Huan L, Chen D, Bao C, et al. miR-192, a prognostic indicator, targets the SLC39A6/SNAIL pathway to reduce tumor metastasis in human hepatocellular carcinoma. *Oncotarget* 2016;7:2672–83.
36. Yan-Chun L, Hong-Mei Y, Zhi-Hong C, Qing H, Yan-Hong Z, Ji-Fang W. MicroRNA-192-5p promote the proliferation and metastasis of hepatocellular carcinoma cell by targeting SEMA3A. *Appl Immunohistochem Mol Morphol* 2015;25:251–60.
37. Morimoto A, Kannari M, Tsuchida Y, Sasaki S, Saito C, Matsuta T, et al. An HNF4alpha-microRNA-194/192 signaling axis maintains hepatic cell function. *J Biol Chem* 2017;292:10574–85.
38. Hsu CH, Hsu CW, Hsueh C, Wang CL, Wu YC, Wu CC, et al. Identification and Characterization of Potential Biomarkers by Quantitative Tissue Proteomics of Primary Lung Adenocarcinoma. *Mol Cell Proteomics* 2016;15:2396–410.
39. Liu D, Yin B, Wang Q, Ju W, Chen Y, Qiu H, et al. Cytoplasmic poly(A) binding protein 4 is highly expressed in human colorectal cancer and correlates with better prognosis. *J Genet Genom* 2012;39:369–74.
40. Pichiorri F, Suh SS, Rocci A, De Luca L, Taccioli C, Santhanam R, et al. Downregulation of p53-inducible microRNAs 192, 194, and 215 impairs the p53/MDM2 autoregulatory loop in multiple myeloma development. *Cancer Cell* 2010;18:367–81.
41. Yang YM, Lee WH, Lee CG, An J, Kim ES, Kim SH, et al. Galna12 gep oncogene deregulation of p53-responsive microRNAs promotes epithelial-mesenchymal transition of hepatocellular carcinoma. *Oncogene* 2015;34:2910–21.
42. Cancer Genome Atlas Research Network, Electronic address: wheeler@bcm.edu, Cancer Genome Atlas Research Network. Comprehensive and integrative genomic characterization of hepatocellular carcinoma. *Cell* 2017;169:1327–41 e23.
43. Kastenhuber ER, Lowe SW. Putting p53 in context. *Cell* 2017;170:1062–78.
44. Wu SY, Rupaimoole R, Shen F, Pradeep S, Pecot CV, Ivan C, et al. A miR-192-EGR1-HOXB9 regulatory network controls the angiogenic switch in cancer. *Nat Commun* 2016;7:11169.
45. Botla SK, Savant S, Jandaghi P, Bauer AS, Mucke O, Moskalev EA, et al. Early epigenetic downregulation of microRNA-192 expression promotes pancreatic cancer progression. *Cancer Res* 2016;76:4149–59.
46. Zhao J, Xu J, Zhang R. SRPX2 regulates colon cancer cell metabolism by miR-192/215 via PI3K-Akt. *Am J Translat Res* 2018;10:483–90.
47. Lin XJ, Chong Y, Guo ZW, Xie C, Yang XJ, Zhang Q, et al. A serum microRNA classifier for early detection of hepatocellular carcinoma: a multicentre, retrospective, longitudinal biomarker identification study with a nested case-control study. *Lancet* 2015;16:804–15.
48. Zhou J, Yu L, Gao X, Hu J, Wang J, Dai Z, et al. Plasma microRNA panel to diagnose hepatitis B virus-related hepatocellular carcinoma. *J Clin Oncol* 2011;29:4781–8.
49. Nguyen CB, Houchen CW, Ali N. APSA Awardee Submission: Tumor/cancer stem cell marker doublecortin-like kinase 1 in liver diseases. *Exp Biol Med* 2017;242:242–9.
50. Ma S, Chan KW, Lee TK, Tang KH, Wo JY, Zheng BJ, et al. Aldehyde dehydrogenase discriminates the CD133 liver cancer stem cell populations. *Mol Cancer Res* 2008;6:1146–53.